

Cathepsin A contributes to left ventricular remodeling by degrading extracellular superoxide dismutase in mice

Mathias Hohl (1), Manuel Mayr (2), Lisa Lang (1), Alexander G. Nickel (1,3), Javier Barallobre-Barreiro (2), Xiaoke Yin (2), Thimoteus Speer (4), Simina-Ramona Selejan (1), Claudia Goettsch (5), Katharina Erb (1), Claudia Fecher-Trost (6), Jan-Christian Reil (1,7), Benedikt Linz (8), Sven Ruf (9), Thomas Hübschle (9), Christoph Maack (1,3), Michael Böhm (1), Thorsten Sadowski (9), Dominik Linz (1,10-12).

- (1) Klinik für Innere Medizin III, Universität des Saarlandes, 66421 Homburg/Saar, Germany
- (2) King's BHF Centre of Research Excellence, The James Black Centre, London SE5 9NU, United Kingdom
- (3) Universitätsklinikum Würzburg, Deutsches Zentrum für Herzinsuffizienz (DZHI), Comprehensive Heart Failure Center (CHFC), Würzburg, Germany
- (4) Klinik für Innere Medizin IV, Universität des Saarlandes, 66421 Homburg/Saar, Germany
- (5) Medizinische Klinik 1, Kardiologie, Universitätsklinikum, Medizinische Fakultät, RWTH Aachen, Germany
- (6) Institut für experimentelle und klinische Pharmakologie und Toxikologie, Universität des Saarlandes, Germany
- (7) Klinik für Innere Medizin II, Universitäres Herzzentrum, 23562 Lübeck, Germany
- (8) Faculty of Health and Medical Sciences, Department of Biomedical Sciences University of Copenhagen, Copenhagen, Denmark
- (9) Sanofi-Aventis Deutschland GmbH, 65926 Frankfurt, Germany
- (10) University Maastricht, Cardiovascular Research Institute Maastricht (CARIM), The Netherlands
- (11) Department of Cardiology, Maastricht University Medical Centre, Maastricht, the Netherlands
- (12) Centre for Heart Rhythm Disorders, Royal Adelaide Hospital, University of Adelaide, Adelaide, Australia

Correspondence:

Dominik Linz, MD, PhD
Maastricht UMC+
Maastricht Heart+Vascular Center
6202 AZ Maastricht
E dominik.linz@mumc.nl
T +31(0)43-3875093 | M +31(0)6-123 99 182

Running title: Cathepsin A degrades extracellular superoxide dismutase

Keywords: cathepsin A; carboxypeptidase; extracellular matrix protein; oxidative stress; extracellular superoxide dismutase; cardiac hypertrophy; cardiac remodeling; left ventricular dysfunction; heart disease; secretome

ABSTRACT

In the heart, the serine carboxypeptidase cathepsin A (CatA) is distributed between lysosomes and the extracellular matrix (ECM). CatA-mediated degradation of extracellular peptides may contribute to ECM remodeling and left ventricular (LV) dysfunction. Here, we aimed to evaluate the effects of CatA overexpression on LV remodeling. A proteomic analysis of the secretome of adult mouse cardiac fibroblasts upon digestion by CatA identified the extracellular antioxidant enzyme superoxide dismutase (EC-SOD) as a novel substrate of CatA, which decreased EC-SOD abundance 5-fold. *In vitro*, both cardiomyocytes and cardiac fibroblasts expressed and secreted CatA protein, and only cardiac fibroblasts expressed and secreted EC-SOD protein. Cardiomyocyte-specific CatA overexpression and increased CatA activity in the LV of transgenic mice (CatA-TG) reduced EC-SOD protein levels by 43%. Loss of EC-SOD-mediated antioxidative activity resulted in significant accumulation of superoxide radicals (WT 4.54 vs. CatA-TG 8.62 $\mu\text{mol}/\text{mg}$ tissue/min), increased inflammation, myocyte hypertrophy (WT 19.8 vs. CatA-TG 21.9 μm), cellular apoptosis, and elevated mRNA expression of hypertrophy-related and pro-fibrotic marker genes, without affecting intracellular detoxifying proteins. In CatA-TG mice, LV interstitial fibrosis formation was enhanced by 19%, and the type I:type III collagen ratio was shifted toward higher abundance of collagen I fibers. Cardiac remodeling in CatA-TG was accompanied by an increased LV weight:body weight ratio and LV enddiastolic volume (WT 50.8 vs. CatA-TG 61.9 μl). In conclusion, CatA-mediated EC-SOD reduction in the heart contributes to increased oxidative stress, myocyte hypertrophy, ECM remodeling, and inflammation, implicating CatA as a potential therapeutic target to prevent ventricular remodeling.

INTRODUCTION

Cardiac function depends on structural and functional integrity of the extracellular matrix (ECM). ECM components are synthesized and secreted by cardiac fibroblasts (CFs) (1) and their proper composition and turnover is controlled by proteolysis (2-4). Degradation of ECM proteins occur either

within the cell after fusion of ECM-containing phagosomes with lysosomes or in the extracellular space by secreted proteolytic enzymes (4). Cathepsins are lysosomal proteases which target a broad range of intra- and extracellular proteins like laminin, fibronectin, elastin and fibrillar collagens (2, 3). Increased activation of cathepsins results in remodeling of subcellular organelles and the ECM, and is associated with cardiac complications including hypertrophic cardiomyopathy, diabetic cardiomyopathy, dilated cardiomyopathy, and myocardial infarction (2, 3). Cysteine protease cathepsins like cathepsin B, K, L and S play pathophysiological roles in cardiac structural changes and progression of heart failure (2, 3). However, the role of the serine protease cathepsin A (CatA) during cardiac disease is unclear. CatA is widely distributed in mammalian tissues, with highest expression found in kidney, lung, endothelium, liver, placenta, and heart (5, 6). Besides its catalytic function as a protease, lysosomal CatA forms a protein complex with neuraminidase 1 and β -galactosidase, which prevents proteolysis of its binding partners thereby regulating and stabilizing lysosomal activity and function (7). In humans, disruption of this protein complex by CatA deficiency or mutations in the gene coding for CatA results in the lysosomal storage disease galactosialidosis (8). CatA is also localized on the cell surface and in the extracellular space, where it has been suggested to be involved in ECM formation, possibly by degradation of extracellular peptides (5, 6, 9). In animal models of myocardial infarction, type 2 diabetes, and angiotensin II-stimulated hypertrophy, cardiac expression of CatA is upregulated, and pharmacological inhibition of CatA-activity exhibited cardio-protective, anti-hypertrophic, and anti-fibrotic effects in these conditions (10-13) but its mechanistic role in cardiovascular disease is unknown.

The present study was designed to identify potential mechanisms of CatA-mediated ECM remodeling processes in the heart using state-of-the-art proteomic analysis of the secretome of adult mouse CFs upon digestion by CatA, and supportive *in vivo* investigations in a transgenic mouse model with cardiomyocyte-specific overexpression of CatA (CatA-TG).

RESULTS

Cathepsin A (CatA) processes extracellular matrix (ECM) proteins. To identify novel ECM-related candidate substrates of CatA, we performed a proteomic analysis of the secretome of adult mouse CFs, which produce and secrete ECM-proteins. Proteins in the conditioned medium of CFs treated with and without human recombinant CatA (n=4 each) were analyzed by Liquid Chromatography Tandem Mass Spectrometry (LC-MS/MS) after filtering using 3kDa columns to recover only small cleavage products rather than intact proteins (14). Using Progenesis® LC-MS software (Non-linear Dynamics), the ion intensities of all detected peptides in the <3kDa fraction were compared between control and CatA-treated CFs (**Fig. 1A**). CatA digestion significantly affected abundance of protein degradation products of collagens (CO5A1 (p=0.001), CO5A2 (p=0.0001), CO3A1 (p=0.002), CO1A1 (p=0.003)) and other ECM proteins (i.e. PGS2 (Decorin; p=0.005), LAMA4 (Laminin Subunit Alpha 4, p=0.028), PGBM (Basement membrane-specific heparan sulfate proteoglycan core protein, also known as perlecan; p=0.025), and FINC (Fibronectin; p=0.002) compared to control. The antioxidant enzyme extracellular superoxide dismutase (SODE or EC-SOD) was one of the most significantly affected extracellular proteins after incubation with CatA (p=0.0001) (**Fig. 1B**, **Table S1 Supporting information**). The proteomics data are also available via ProteomeXchange with identifier PXD019895). EC-SOD is an essential antioxidant enzyme, which is exclusively located in the ECM, catalyzing the dismutation of superoxide to hydrogen peroxide and oxygen (15). Three fragment peptides and possible cleavage sites were detected for EC-SOD in control conditions but were undetectable upon treatment with CatA (**Fig. 1C**). This finding added a novel and highly relevant aspect on the role of CatA in cardiac disease, because EC-SOD provides the only direct defense-mechanism against superoxide radicals within the ECM (15) and CatA-mediated loss of

antioxidant protection may facilitate ECM remodeling.

Differential expression pattern of cathepsin A (CatA) and extracellular superoxide dismutase (EC-SOD) in cardiomyocytes (CMs) and cardiac fibroblasts (CFs). An initial gene expression analysis comparing isolated primary adult mouse CFs with CMs demonstrated mRNA transcription of CatA in both cell lines, whereas EC-SOD mRNA was only detectable in CFs (**Fig. S1 Supporting information**). These mRNA data were confirmed at the protein level by analyzing cultured neonatal rat CMs and rat CFs. While CatA protein was expressed and secreted by both cell types (**Fig. 2A and 2B**), the presence and secretion of EC-SOD protein was only evident in CFs (**Fig. 2C and 2D**).

Cardiomyocyte-specific cathepsin A (CatA) overexpression in mice results in posttranslational downregulation of extracellular superoxide dismutase (EC-SOD), increased oxidative stress and enhanced inflammation in the left ventricle (LV). To further understand the function of CatA in ECM remodeling *in vivo*, transgenic mice with a cardiomyocyte-specific postnatal overexpression of active human CatA were generated (CatA-TG) using the alpha myosin heavy chain promoter (**Fig. S2 Supporting information**). CatA-TG mice developed normally and showed no apparent abnormal phenotype. Quantitative Real-Time PCR, Western blot analysis and immuno-histological staining confirmed overexpression of human CatA in the myocardium of CatA-TG mice (**Fig. 3A-C**).

Detoxification of reactive oxygen species (ROS) are catalyzed by anti-oxidative enzymes, including catalase and superoxide dismutases (SODs). Beside the extracellular isoform EC-SOD, two intracellular isozymes of SODs exist, comprising cytosolic Cu/Zn-SOD (SOD1) and mitochondrial Mn-SOD (SOD2) (15). Western blot analysis demonstrated that overexpression of CatA did not affect protein expression of catalase, SOD1 and SOD2 which are located within the cell. (**Fig. 3D and 3E**). Using an EC-SOD antibody that specifically targets the N-terminal region demonstrated a significant reduction of EC-SOD protein in the LV of CatA-TG compared to their wild type littermate controls (WT) (**Fig. 3D, 3E**). Interestingly, EC-

SOD mRNA levels were unaltered (**Fig. 3F**), strongly suggesting a posttranslational regulation, i.e. consistent with proteolysis of EC-SOD.

To characterize downstream consequences of reduced EC-SOD and its loss of antioxidant protection (15), we determined the levels of superoxide radicals in LV tissue of CatA-TG and in WT mice. Using electron spin resonance spectroscopy measurements, CatA-TG mice demonstrated increased LV oxidative stress, as indicated by accumulation of superoxide radicals (**Fig. 4A**). Oxidative stress was associated with elevated gene expression of connective tissue growth factor (CTGF), an important redox-sensitive inducer of fibrosis (16) (**Fig. 4B**). Increased gene expression of tumor necrosis factor alpha (TNF α), interleukin 6 (IL6), and interleukin 2 (IL2) as well as repressed transcription of interleukin 10 (IL10) demonstrated an enhanced inflammatory response in CatA-TG mice (**Fig. 4C**). Interleukin 1 beta (IL1b) was not regulated. Of note, mRNA levels of IL2 and IL10 were considerably lower compared to gene expression of TNF α or IL6, and immunohistological stainings for infiltration of macrophages or neutrophils in the heart of CatA-TG and WT mice showed no significant inflammatory infiltration (**Fig. S3. Supporting information**). CatA-TG demonstrated a higher proportion of apoptotic cells, as detected by TUNEL (terminal deoxynucleotidyl transferase dUTP nick end labeling) staining (**Fig. 4D**), independent of a differential expression of pro-enzyme caspase 1 and caspase 3 protein (caspase 1 protein: WT: 1.00 \pm 0.20 vs. CatA-TG: 1.25 \pm 0.61, $p=0.261$; caspase 3 protein: WT: 1.01 \pm 0.22 vs. CatA-TG: 1.24 \pm 0.31, $p=0.098$) and in the absence of active caspase subunits (**Fig. S4. Supporting information**). LV protein expression of NAD(P)H oxidase 2 (Nox2/gp91phox), Nox4 and xanthine oxidase, representing major sources of cellular ROS (17), were unchanged between WT and CatA-TG (Nox2 protein: WT: 1.00 \pm 0.20 vs. CatA-TG: 1.06 \pm 0.32, $p=0.611$; Nox4 protein: WT: 1.00 \pm 0.09 vs. CatA-TG:

1.16 \pm 0.35, $p=0.420$; Xanthine oxidase protein: WT: 1.00 \pm 0.10 vs. CatA-TG: 1.09 \pm 0.27, $p=0.352$; **Fig. S5 Supporting information**).

Cathepsin A transgenic mice (CatA-TG) demonstrate left ventricular (LV) structural and functional remodeling. Body weight did not differ between wild type controls and CatA-TG mice (WT: 35.4 \pm 4.4 vs. CatA-TG: 33.5 \pm 5.2 g; $n=15$ each; $p=0.304$). Heart weight to body weight ratio ($n=15$ each) (**Fig. 5A**), as well as LV weight to body weight ratio was significantly increased (WT: 3.27 \pm 0.19 vs. CatA-TG 4.29 \pm 0.56 mg/g; $n=6$; $p=0.0019$), and LV cardiomyocyte diameter was enlarged ($p=0.024$) (**Fig. 5C**). Gene expression of hypertrophy marker atrial natriuretic peptide (ANP) and brain natriuretic peptide (BNP) were elevated in CatA-TG mice compared to their wild type littermate controls (**Fig. 5D**). CatA-TG mice also demonstrated increased LV interstitial fibrosis formation (**Fig. 6A and 6C**) and a shift in the ratio of collagen type I (red-yellow fibers) to collagen type III (green fibers) as assessed by polarized light microscopy (**Fig. 6B and 6D**). In the LV of CatA-TG mice mRNA-expression of pro-fibrotic transforming growth factor beta 1 (TGF β -1) and of the ECM components collagen 1a2 (Col1a2), Col3a, Col5a1, fibronectin (FN) and ECM stabilizing protein lysyl oxidase (Lox), which catalyzes cross-linking of collagen fibrils and elastin (18), were elevated (**Fig. 6E**). The development of perivascular fibrosis in the heart was unaffected by cardiomyocyte-specific cathepsin A overexpression (WT: 31.3 \pm 5.9 vs. CatA-TG: 34.3 \pm 5.4 % $p=0.398$; **Fig. S6. Supporting information**). To assess LV function in this unchallenged phenotype of CatA-TG, we used an isolated working heart preparation to measure functional parameters under standardized hemodynamic conditions. At 6 months of age isolated CatA-TG hearts demonstrated significant increased LV enddiastolic volume (LVEDV) (WT: 50.8 \pm 5.8 vs. CatA-TG: 61.9 \pm 6.2 μ l; $p=0.018$), while other functional parameters were unchanged (**Table 1**). Noteworthy, CatA-TG mice developed a significantly increased left ventricular endsystolic pressure at an age of 18 months (**Fig. S7. Supporting information**).

DISCUSSION

The composition and turnover of the ECM is tightly controlled by proteolysis (2-4). Pathophysiological remodeling of the ECM contributes critically to LV dysfunction and progression of heart failure (19, 20). Here, we provide new evidence for the involvement of the serine carboxypeptidase CatA in the degradation of the extracellular antioxidant enzyme EC-SOD and regulation of subsequent ECM remodeling processes. These findings highlight proteolysis as a potential target in cardiovascular diseases and heart failure.

Proteomic analysis of the secretome of adult mouse CFs identified EC-SOD as a novel target and substrate of CatA at slightly acidic pH5.5. As a multifunctional enzyme, CatA exhibits a strong carboxypeptidase activity in an acidic milieu and a de-amidase as well as a weakened enzymatic carboxypeptidase activity at neutral pH (5, 6, 21).

At neutral pH, the ECM is protected against extracellular degradation by secreted or membrane-bound cathepsins. However, in the LV myocardium of CatA-TG mice the imbalanced expression pattern of pro- and anti-inflammatory marker genes suggests an inflammatory state. Under inflammatory conditions acidification of the peri- and extracellular space increases the proteolytic activity of cathepsins and further promotes the secretion of lysosomal proteases. Moreover, within the ECM the acidic pH facilitates the processing of secreted inactive pro-cathepsins into catalytically active mature proteases (22). Additionally, binding of cathepsins to heparin or heparan sulfate has been shown to stabilize its enzyme structure and potentiate peptidase activity even at alkaline pH (23). Taken together, these factors may regulate CatA activity to hydrolyze its target proteins after secretion into the interstitial space (6, 7, 21).

EC-SOD represents the main defense-mechanism in the ECM against oxidative stress and is the only extracellular enzyme detoxifying superoxide radicals (15). EC-SOD is anchored to the cell surface and the ECM via its C-terminal region, known as the heparin-binding domain. The heparin-binding domain determines the binding affinity for its ligands including cell surface heparan sulphate proteoglycans, heparin, and type I collagen (15, 24, 25), thus tightly regulating distribution of EC-SOD in the ECM. Interaction of EC-SOD with ECM-components like collagen and

syndecan-1 shield its bindings-partners from oxidative damage, preventing ECM remodeling and attenuate inflammatory responses (15, 25). Subsequently, EC-SOD depletion reduces antioxidant protection leading to fragmentation of ECM-components, oxidant-induced fibrosis formation, and myocyte hypertrophy (15, 25, 26).

Here, we demonstrated that both CFs and CMs express and secrete CatA, while EC-SOD is exclusively expressed and secreted by CFs, but not by CMs. In our transgenic mouse model, cardiomyocyte-specific overexpression of CatA induced a significant decrease of LV EC-SOD protein levels. As CMs do not express EC-SOD, our findings suggest a CatA-mediated degradation of EC-SOD protein within the ECM and exclude intracellular digestion of EC-SOD in CMs. Additionally, LV EC-SOD mRNA expression was not affected in CatA-TG mice which indicates a posttranslational depletion of EC-SOD protein in the ECM.

Oxidative stress highly contributes to the development of cardiac hypertrophy and fibrosis (17). In CatA-TG mice, reduction of EC-SOD was associated with increased oxidative stress, elevated expression of the redox-sensitive pro-fibrotic CTGF (16) and development of a hypertrophic and pro-fibrotic phenotype with increased LV weight and elevated LVEDV, known hallmarks for heart failure (summarized in **Figure 7**). Comparable phenotypes have been described previously in EC-SOD knockout mice (25, 26, 27, 28). Lack of EC-SOD was associated with exacerbated oxidative stress-induced myocardial apoptosis, LV fibrosis formation and inflammatory cell infiltration, demonstrating an important protective role of EC-SOD against extracellular oxidative stress (25, 26, 27, 28). Vice versa, overexpression of EC-SOD reduced interstitial fibrosis and ventricular dysfunction in a murine model of ischemic cardiomyopathy (29).

In the failing heart, major sources of cellular ROS comprise the xanthine oxidase and NAD(P)H oxidases (like Nox2 and Nox4). Dysregulation of these enzymes is involved in cardiovascular disease, hypertension and heart failure (17). However, in CatA-TG mice, increased superoxide radicals could not be linked to a differential expression of cellular ROS-producing oxidases. Therefore, ECM

remodeling in CatA-TG is likely a consequence of CatA-mediated loss of antioxidant protection and subsequent accumulation of extracellularly derived ROS in the ECM.

A recent proteomic profiling analyzed the impact of a pharmacological inhibition of CatA in a mouse model of myocardial-infarction (MI), demonstrating a partial rescue of left ventricular proteome-alterations associated with MI and attenuated elevated levels of cardiac stress response proteins (13). Furthermore, a quantitative proteome comparison of whole heart lysates from CatA transgenic mice and their littermates linked CatA to cardiac oxidative stress response, and CatA-overexpression in cultured rat cardiomyoblasts resulted in higher sensitivity to oxidative stress (30).

Potential limitations of this study are as follows: Secretome analysis and transgenic overexpression in mice might not recapitulate physiological levels or cell-type specific expression patterns. While certain proteins may be inaccessible to the protease in a tissue environment, proteomics returned a plethora of other potential substrates of CatA, including decorin. Processed forms of decorin protein core have been shown to regulate the local bioavailability of pro-fibrotic growth factors, like CTGF (31). Analysis of our proteomics data also indicated a possible participation of CatA in the processing of other structural ECM proteins, which may have contributed to the cardiac phenotype observed in CatA-TG mice. A comparable ECM-proteolytic activity involving the degradation of laminin, fibronectin, elastin and fibrillar collagens has also been described for the larger family of cysteine-cathepsins (2, 3). Although our findings in CatA-TG mice are consistent with digestion of EC-SOD by CatA, future biochemical studies are needed to investigate whether CatA degrades ECM proteins directly or via other intermediate molecules being activated or inhibited by CatA.

CONCLUSION

The present study sheds first light on a previously unrecognized role of CatA outside the lysosome in the proteolysis of the extracellular antioxidant enzyme EC-SOD. In

the heart, CatA-mediated reduction of EC-SOD levels resulted in oxidative stress due to insufficient removal of reactive oxygen species. Thus, EC-SOD degradation represents a plausible link between CatA activation and LV ECM remodeling and implicates CatA as a potential therapeutic target to prevent cardiac ECM remodeling.

EXPERIMENTAL PROCEDURES

Study approval - All animal studies were performed in accordance to the German law for the protection of animals. The investigation conforms with “The guide for the care and use of laboratory animals” published by the United States National Institutes of Health (Eighth edition; revised 2011), the Declaration of Helsinki and was approved by the local animal ethics committee of the University of the Saarland (#21/2014).

Identification of candidate substrates of cathepsin A (CatA) by a proteomics approach

Five-week old male C57BL/6N mice (n=4) were anesthetized with 5% isoflurane in 95% O₂ and sacrificed by intraperitoneal (i.p.) injection of ketamine hydrochloride (100mg/kg body weight) and xylazine hydrochloride (10mg/kg body weight). Isolation and culture of primary cardiac fibroblasts (CFs): Primary mouse CFs were isolated from the hearts of 5 weeks old male C57BL/6N mice (n=4). Hearts were extracted, washed and diced into small pieces, carefully washed in ice-cold phosphate buffered saline (PBS, Sigma-Aldrich) to remove plasma contaminants. The pieces were pre-digested in collagenase II solution (5mg/mL) for 10min. The collagenase II solution was replaced and the tissue pieces were incubated for 45min-60min at 37°C. The digested tissue pieces were washed in complete medium (DMEM supplemented with 10% FBS, 2mM L-glutamine, 100U/mL penicillin, 100ug/mL streptomycin) before plating. CFs were cultured on 0.1% gelatin-coated T25 flasks in complete medium at 37°C in a humidified incubator with 5% CO₂ until 80% confluence. Cells were washed 3 times with serum-free medium then incubated in serum-free medium for 3 days. The conditioned medium was centrifuged at 4000rpm (3200 x g) for 10min to remove cell debris. The supernatants were transferred into new tubes and stored at -80°C until further analysis.

Digestion by CatA: For digestion with CatA, conditioned media were concentrated and the buffer was exchanged to assay buffer (25mM MES, 5mM DTT, pH=5.5) with 3KDa MWCO spin column (Merck Millipore). Control samples (n=4) were incubated in buffer with protease inhibitor only (for inhibition of endogenous proteases other than CatA). Treated samples (n=4) were incubated in buffer with protease inhibitor only (for inhibition of endogenous proteases other than CatA) plus human recombinant CatA (1µg/mL, Sanofi-Aventis, Deutschland) (10). Both groups were incubated at 37°C for 24 hours with agitation (reaction took place inside the spin column). After reaction, the samples were centrifuged. The degradation products in the <3kDa fractions were collected and purified with C18 spin columns (Thermo Fisher Scientific). Analysis by Liquid Chromatography Tandem Mass Spectrometry (LC-MS/MS): Peptides were analyzed by LC-MS/MS as previously described (32, 33). Peptides were separated by reverse phase chromatography (Acclaim PepMap100 C18, 75µm Å x 25cm) on a nanoflow LC system (Ultimate3000 RSLCnano, Thermo Fisher Scientific) equipped with a trap column (Acclaim PepMap100 C18, 300µm Å x 5mm). The chromatographic separation was performed with a mobile phase of HPLC grade water containing 2% acetonitrile and 0.1% formic acid (eluent A) and a mobile phase of 80% acetonitrile, 20% HPLC grade water and 0.1% formic acid (eluent B) with a 70-minute gradient (2% to 10%B in 3 minutes, 10% to 30%B in 34 minutes, 30% to 40%B in 3 minutes, 99%B for 10 minutes, 2%B for 20 minutes) at a flow rate of 350 nL/min. The column was coupled to an LTQ OrbitrapXL mass spectrometer (Thermo Fisher Scientific) with a nanospray source (Picoview, New Objective, Inc.). The mass spectrometry acquisition involved 1 full MS scan over a mass-to-charge range encompassing m/z 400–1600 using the Orbitrap analyzer, followed by data-dependent collision-induced dissociation MS/MS scans of the 6 most intense ions detected in the full scan, with dynamic exclusion enabled and rejection of singly charged ions. The data were analysed using Progenesis LC-MS software (version 4.1, Nonlinear Dynamics). Peaklist of MS2 spectra from features with intensity > 2-fold change, $p < 0.05$ between the CatA treated group and

control group was exported and identified by Mascot (Matrix Science; version 2.3.01) with the following parameters: enzyme: none; database: UniProt/SwissProt mouse database (release 2012_03, 16520 protein entries); precursor mass tolerance: 10ppm; fragment mass tolerance: 0.8Da; fixed modification: none; variable modification: none. Search results were loaded back to Progenesis to match with the significantly changed features. Peptides with Mascot score > 10 were used for quantification and final protein table was exported (Supplemental Table 1).

Isolation of primary adult mouse cardiomyocytes and cardiac fibroblasts for gene expression analysis - Isolation of adult mouse cardiac fibroblasts (CFs) and cardiomyocytes (CMs) was described elsewhere (34, 35). In short: Six-week old male C57BL/6N mice (n=10) were anesthetized with 5% isoflurane in 95% O₂ and sacrificed by intraperitoneal (i.p.) injection of ketamine hydrochloride (100mg/kg body weight) and xylazine hydrochloride (10mg/kg body weight). To isolate primary mouse CFs, hearts were extracted, washed and diced on ice into small pieces, and carefully washed in ice-cold phosphate buffered saline (1xPBS: 137mmol/L NaCl, 2.7mmol/L KCl, 10mmol/L Na₂HPO₄, 1.8mmol/L KH₂PO₄). The pieces were transferred to a sterile glass beaker and digested using a 25 ml collagenase II digestion-solution (100U/ml collagenase II (#LS004176; Worthington) in Hanks balanced salt solution (HBSS) buffer (0.137 M NaCl, 5.4mM KCl, 0.25mM Na₂HPO₄, 0.1g glucose, 0.44mM KH₂PO₄, 1.3mM CaCl₂, 1.0mM MgSO₄, 4.2mM NaHCO₃) and 2.5% Trypsin (#L2133, Merck Millipore) under constant stirring at 37°C for 10 min. Supernatant was collected in a 50 ml falcon tube containing 2 ml complete medium (M199 + GlutaMax (Gibco, #41150-020) supplemented with 10% FBS (Gibco, #16170-07), 100 U/mL penicillin, 100 µg/mL streptomycin (Gibco, #15140-122)). Digestion was repeated 10 times until tissue was completely dissolved. Cardiomyocytes were collected by sedimentation for 8-10 minutes and the pellet was snap-frozen in liquid nitrogen for subsequent RNA-isolation. Supernatants were collected as described and CFs were pelleted by centrifugation for 5 min at 300 x g at 4°C. CFs were cultured on 6-well tissue culture dishes (VWR, TPPA92006) in

complete medium at 37°C in a humidified incubator with 5% CO₂ until 80% confluence. mRNA was isolated from mouse CMs and mouse CFs using peqGold TriFast (#30-2010; PeqLab) extraction reagent following the manufacturer's protocol.

Isolation of primary neonatal rat cardiac myocytes and cardiac fibroblasts - Neonatal rat CMs and CFs were isolated from 5 days old Sprague-Dawley rat hearts (Charles River, Germany) of mixed sex. Hearts were removed, the ventricles dissected and digested in ADS buffer containing (in mmol/L) NaCl 116, HEPES 20, Na₂HPO₄ 0.8, Glucose 5.6, KCl 5.4 and MgSO₄ x 7 H₂O 0.8, pH 7.35, 0.6mg/ml Pankreatin (Sigma, P-3292) and 0.5 mg/ml Collagenase Type 2 (Worthington Biochemical; #LS004176) at 37°C in a water bath with constant stirring at 80-100rpm for 5min. Supernatant (not tissue) was transferred in a 50 ml Falcon tube containing 2 ml neonatal calf serum (NCS; Gibco #16010-159) to stop enzymatic reaction. Procedure was repeated 6 times, all supernatants were collected and the cells were pre-plated on 6-Well plates (Falcon #353846, BD, Franklin Lakes, NJ, USA) in F10 medium (Gibco; +10% horse serum, 5% FCS and 1% penicilline/streptomycine) to allow separation of cardiac fibroblasts by adhesion. After 45 min, the still-suspended neonatal cardiomyocytes were removed from the attached cardiac fibroblasts, counted (Neubauer counting chamber) and plated at a density of 1.65 – 1.75 x 10⁶ cells per 60 mm culture dish (#93060, TPP, Switzerland) in complete F10 medium at 37°C in a humidified incubator with 5% CO₂ until 80% confluence. The attached neonatal cardiac fibroblasts were grown in Dulbecco's modified Eagle's medium supplemented with 10% (v/v) fetal calf serum, gentamicin (0.08mg/ml), and penicillin (100IU/ml) at 37°C in a humidified incubator with 5% CO₂ until 80% confluence. Afterwards both cell lines were kept in serum-free medium for 48h. Medium and cells were harvested and stored at -80°C until further processed.

CatA-transgenic mice (CatA-TG)-mouse model: For the generation of transgenic mice that overexpress the human CatA specifically in cardiomyocytes a vector containing the mouse alpha MHC promoter (5.7kb) driving the human CatA minigene (cDNA clone ID:

CLN16325899) was constructed and described elsewhere (11). Kozak translation initiation sequence and SV40pA (249bp) was introduced to enhance transgene expression. LoxP-hUBp-em7- neo-loxP cassette (2648 bp) was inserted downstream of stop codon for selection. VelociMouse® technology (Regeneron) was used to target embryonic stem cells and microinject them into mouse embryos (For details refer to reference article (11, 36)). In brief, F1H4 (129S6SvEv/C57BL6F1) embryonic stem cells were electroporated with the linearized vector construct and positive clones were microinjected into 8-cell stage mouse C57BL/6N embryos. Pseudopregnant recipient female mice were anesthetized with Avertin (2,2,2-tribromoethanol; Fluka 90710, Aldrich Chemical) 2.5% in tert-amyl alcohol administered i.p. at a dose of 0.1 ml/10 g body weight and embryos were transferred to uteri by microinjection, weaned pups were scored, and high percentage chimera males were selected for mating with flp-positive C57B/L6N females to remove the selection cassette, to prove germ-line transmission, and to generate F1 animals for further breeding. Hemizygote animals were identified by genomic tail DNA probed with PCR primers 5'-AATCTCTATGCCCCGTGTGC-3' (F) and 5'-GGCAGGCGAGTGAAGATGTT-3' (R). The copy number of the transgene (4 copies) was estimated by a quantitative PCR assay for the inserted transgene that determines the normalized average difference in threshold cycle among the transgenic ES cell clones and the mice derived from them. Mice were kept and bred under specific pathogen-free conditions (SOPF) in the animal care facility.

Working heart - Working heart experiments with isolated hearts of six months old male CatA-TG mice and their male littermates were performed as previously described (37). Mice were anesthetized with 5% isoflurane in 95% O₂ and sacrificed by intraperitoneal (i.p.) injection of ketamine hydrochloride (100mg/kg body weight) and xylazine hydrochloride (10mg/kg body weight). The aorta was cannulated with an 18-G metal cannula for a Langendorff retrograde perfusion mode (baseline, 80mmHg perfusion pressure) with Krebs-Henseleit buffer (KHB) in a working heart apparatus (IH-SR Perfusion system type 844/1 Hugo Sachs Elektronik). After establishing coronary perfusion in the

Langendorff mode, “working heart” preparation was continued by cannulating the left atrium through the pulmonary vein with a 16-G steel cannula. This cannula was connected to a preload column, which was water-jacketed and heated to 38°C, resulting in a myocardial temperature of 37°C when the heart was operating in the working mode (preload 10mmHg, afterload 60mmHg). Two platinum pacing electrodes embedded in polyester resin were attached to the right atrium to pace the hearts at about 400bpm. LV systolic and diastolic function was recorded via a high fidelity pressure-conductance catheter (Millar 1.4 F SPR-835, Millar) inserted into the LV cavity through a small puncture in the apex made with a 22 1/4 gauge needle. Cardiac inflow and aortic flow were recorded continuously by inline ultrasonic transit time probes and these measurements were used to calibrate volume measurement of the conductance catheter signal gain. Parallel conductance (conductance signal offset) was determined by the saline dilution method by injecting a 5ml bolus of hypertonic (5%) saline into the left atrial cannula, causing a transient change in the conductivity of KHB in LV cavity.

Detection of superoxide using electron spin resonance spectroscopy - Production of superoxide in the left ventricle was measured using electron spin resonance (ESR) spectroscopy as described previously (38). Briefly, left ventricular tissue was placed in Krebs-HEPES buffer containing 25µmol/L deferoxamine (Noxygen) and 5µmol/L diethyldithiocarbamic acid (DETC, Noxygen) and incubated with 1-hydroxy-3-methoxycarbonyl-2,2,5,5-tetramethylpyrrolidine (CMH, 500µmol/L) as spin trap for one hour. ESR spectra were recorded using a Bruker e-scan spectrometer (Bruker Biospin) with the following settings: center field 1.99g, microwave power 20mW, modulation amplitude 2 G, sweep time 60s, field sweep 60 G.

Histology and immunohistochemical staining - Hearts were rapidly removed, trimmed free from non-cardiac tissues and weighed. Thereafter, the heart was fixed in buffered 4% formaldehyde for 24h and imbedded in paraffin for histological evaluation. Tissue sections of 4µm were fixed at 56°C overnight,

deparaffinized, rehydrated and stained with hematoxylin and eosin (HE) (Hematoxylin: #10228.01000, Morphisto GmbH, Frankfurt am Main, Germany and Eosin Y; #1.15935.0025, Merck, Darmstadt, Germany) to determine cardiomyocyte diameter. To visualize tissue fibrosis amount, the sections were stained with Picro-Sirius Red (#13422.00500, Morphisto GmbH, Germany). The percentage of the LV consisting of interstitial collagen was calculated as the ratio of Picro-Sirius Red positively stained area over total LV tissue area, excluding blood vessels and the epi- and endocardial plane. For LV stained with Picro-Sirius Red, polarization microscopy was performed to visualize collagen type I (yellow-red fibers) and type III (green fibers) based on the birefringence properties of collagen (39). Perivascular fibrosis was evaluated as the ratio of fibrosis surrounding the vessel wall to total vessel area. For the analysis Nikon Instruments Software (NIS)-Elements (BR 3.2, Nikon instruments) was used.

For immunostaining of CatA, heart tissue was fixed in buffered 4% formaldehyde for 24h and imbedded in paraffin for histological evaluation. Tissue sections of 4µm were mounted on glass slides, deparaffinized with xylene and hydrated in descending concentrations of ethanol. Following hydration, sections were incubated for 1 hour in 0.05% Citraconic anhydrid (Sigma-Aldrich) at 98°C in a water bath and washed afterwards in 1xPBS-Tween (Phosphate-Buffered Saline: 137mmol/L NaCl; 2.7mmol/L KCl; 4.3mmol/L Na₂HPO₄; 1.47mmol/L KH₂PO₄, pH7.4 containing 0.1% Tween) for 10 minutes at room temperature. Slides were incubated with anti-cathepsin A antibody (R&D Systems #AF1049; dilution 1:30) in 1xPBS-Tween overnight in a moisture-chamber at 4°C. Sections were washed 3x5 minutes with 1xPBS-Tween and secondary antibody (biotin-labeled anti-goat-IgG, dilution 1:30) was added for 2hours and incubated in the moisture-chamber at 37°C. Slides were washed 3x5 minutes with 1xPBS-Tween and incubated with a tertiary streptavidin-peroxidase antibody (#SA202; Chemicon/Millipore) in 1xPBS-Tween and incubated for 20min in a moisture-chamber. After washing as before, slides were incubated shortly with AEC-chromogen (DAKO; #K3464) at room temperature and rinsed with Aqua dest. followed by staining with

hematoxylin for 5min and blued with tap water for 15min to allow staining. Slides were mounted with Aquatex (Merck) and analyzed.

TUNEL assay - To assess the amount of apoptotic cells we performed TUNEL (terminal deoxyribonucleotidyl transferase (TdT)-mediated dUTP nick end labeling; ApopTag®, Chemicon) assay following the manufacturer's protocol. In short: Tissue sections of 4µm were mounted on glass slides, deparaffinized with xylene and hydrated in descending concentrations of ethanol. Slices were treated with proteinase K solution (20µg/ml) for 30min and washed twice with bi-distillated water (ddH₂O). Afterwards, slices were incubated with 3% hydrogen peroxide solution for 5min, washed twice with phosphate buffered saline solution (1xPBS: 137mmol/l NaCl; 2.7mmol/l KCl; 4.3mmol/l Na₂HPO₄; 1.47mmol/l KH₂PO₄, pH 7.4) and incubated with "Working Strength TdT Enzyme" solution for 60min at 37°C in a moisture-chamber. Slices were washed for 10min with a "Stop/Wash" buffer and incubated with anti-digoxigenin conjugate peroxidase for 30min. Afterwards slices were stained with AEC-chromogen (3-amino-9-ethylcarbazole; #K3464 DAKO), washed with ddH₂O, and staining with hematoxylin for 5min and blued with tap water for 15min to allow staining. Slides were afterwards mounted with Aquatex (Merck) and analyzed.

For immunostaining of F4/80 and Ly-G6, heart tissue was fixed in buffered 4% formaldehyde for 24h and imbedded in paraffin for histological evaluation. Tissue sections of 4µm were mounted on glass slides, deparaffinized with xylene and hydrated in descending concentrations of ethanol. Slides were washed with Aqua dest for 1 minute and incubated in 3% H₂O₂ (diluted in Aqua dest.) for 5 minutes, then rinsed again in Aqua dest. and incubated at 95°C for 20 minutes in 0.01 mol/L sodium citrate buffer (pH 6.0) containing 0.05% Tween 20. After 10 minutes cooling, slides were washed twice with Aqua dest. followed by 1xPBS (Phosphate-Buffered Saline: 137mmol/L NaCl; 2.7mmol/L KCl; 4.3mmol/L Na₂HPO₄; 1.47mmol/L KH₂PO₄, pH 7.4) for 5 minutes at room temperature. Afterwards slides were incubated for 30 minutes in TNB buffer (0.1 mol/L Tris-HCL (pH 7.5) containing 0.15 mol/L NaCl and 0.5% blocking reagent (Perkin Elmer #FP1020)) at room temperature. After

removal of TNB buffer primary antibodies were incubated over night at 4°C (Anti-mouse F4/80, eBioscience, #14-4801, diluted 1:50 in TNB buffer. Anti-mouse Ly-6G (Gr-1), eBioscience, #14-5931, diluted 1:50 in TNB buffer) for at least 15 hours, followed by 1 hour incubation at 37°C. Slides were washed twice with 1xPBS for 5 minutes and incubated with secondary antibody conjugated to biotin (Santa Cruz, sc-2041, diluted 1:200 in TNB buffer) for 30 minutes. Slides were washed twice with 1xPBS for 5 minutes and incubated with labeled streptavidin-HRP antibody (Perkin Elmer #FP1047), diluted 1:100 in TNB buffer) for 30 minutes, washed as before and incubated for 10 minutes with biotinyl tyramide diluted (Perkin Elmer #FP1019) at 1:50 in amplification diluent (Perkin Elmer #FP1050). After washing twice with 1xPBS for 5 minutes, slides were incubated in SA-fluorophore (Texas red streptavidin, Vector laboratories #SA-5006, diluted 1:50 in HEPES buffer) for 30 minutes at 37°C. After washing twice with 1xPBS for 5 minutes slides were covered with DAPI containing mounting medium (Vector laboratories, Vectorshield, #H-1500) and analyzed.

Polymerase Chain Reaction (PCR) - Gene expression analysis was performed by real-time PCR. Total RNA was extracted from left ventricular tissue of mouse using peqGold TriFast (#30-2010; PeqLab) extraction reagent per manufacturer's protocol. Genomic DNA impurities were removed by DNase treatment (Peqlab), and cDNA was synthesized by reverse transcription using the HighCap cDNA RT Kit (#4368814; Applied Biosystems) according to the manufacturer's protocol. TaqMan PCR was conducted in a StepOne plus thermocycler (Applied Biosystems) using TaqMan GenEx Mastermix (#4369016, Applied Biosystems). Signals were normalized to corresponding glyceraldehyde-3-phosphate dehydrogenase (GAPDH) controls. No template controls were used to monitor for contaminating amplifications. The ΔC_t was used for statistical analysis and $2^{-\Delta\Delta C_t}$ for data presentation. Mouse probes used to amplify the transcripts were as follows (purchased by Applied Biosystems Life Technologies): GAPDH (Mm99999915_g1) cathepsin A (Mm00447197_m1), TGFb1 (Mm03024053_m1), CTGF (Mm01192931_g1), Col5a1

(Mm00489342_m1), Colla2
(Mm01165187_m1), Col3a1
(Mm01254476_m1), fibronectin 1
(mm01256734_m1), Lox (Mm00495386_m1),
ANP (Mm01255747_g1), BNP
(Mm01255770_g1), EC-SOD (Sod3:
Mm01213380_s1), TNFalpha
(Mn00443258_m1), interleukin 6
(Mm00446190_m1), interleukin 2
(Mm00434256_m1), interleukin 10
(Mm00439614_m1), interleukin 1 beta
(Mm00434228_m1), Bcl-2
(Mm00477631_m1), Bak-1
(Mm00432045_m1), Bax (Mm00432051_m1),
alpha MHC (Mhy6: Mm00440359_m1), Neu1
(Mm00456846_m1), lamp1
(Mm00495262_m1). For analysis of human
cathepsin A: Hs00264902_m1 (CTSA).

Western blot analysis - Isolated cardiomyocytes and cardiac fibroblasts, as well as left ventricular tissue were homogenized in lysis buffer (Tris-HCl 100mmol/L, Sodium dodecyl sulfate (SDS) 4%, glycine 20%) containing complete protease inhibitors (#11873580001; Roche) and 1mM PMSF and centrifuged at 16.000g for 10 min. 50µg of protein was separated on 10% SDS-PAGE and electrophoretically transferred to nitrocellulose membranes (0.2µm pore size, Schleicher and Schuell). Membranes were blocked in Tris-buffered saline (TBS) containing 5% nonfat dry milk for at least 120min at room temperature and exposed to the following primary antibodies overnight: anti-glyceraldehyde-3-phosphate dehydrogenase (GAPDH; Millipore, MAB374), anti-superoxide dismutase-1 (SOD1; Santa Cruz Biotechnology, sc-11407); anti-superoxide dismutase 2 (SOD2; Santa Cruz Biotechnology, sc-30080), anti-superoxide dismutase 3 (EC-SOD, SOD3, Santa Cruz Biotechnology, sc-32222), anti-rat SOD3 (rat EC-SOD, R&D Systems, AF4817) Anti-cathepsin A (R&D Systems, AF1049), and for rat Anti-CTSA (Sigma life science, HPA031068), anti-Collagen 1a2 (Santa Cruz Biotechnologies, sc-393573), Anti-Catalase (Cell Signaling Technology, #14097), Anti-Nox2/gp91phox [ERP6991] (abcam; ab129068), Anti-NADPH oxidase 4 (abcam ab154244), Anti-xanthine oxidase (Santa Cruz Biotechnologies, sc-398548), Anti-Caspase 3 (Cell Signaling Technology, #9662), Anti-Caspase 1 (Cell Signaling, #24232), Anti-Bcl-2 (Santa Cruz Biotechnology, sc-492), Anti-Bax

(Santa Cruz Biotechnology, Sc-7480). Respective secondary antibodies (purchased from Sigma: anti-mouse: #A5278, anti-rabbit: #A6154, anti-goat: A5420) were incubated for 60min at room temperature. Proteins were visualized by enhanced chemiluminescence according to the manufacturer's guidelines (#RPN2106, Amersham Pharmacia Biotech) and analyzed using the Fusion SL gel documentation system (Peqlab). Data are presented as intensity optical density (IOD).

Cathepsin A activity assay - CatA activity was measured using the fluorogenic peptide substrate V (R&D Systems; #ES005) according to the manufacturer's protocol. Degradation of the fluorogenic peptide substrate Mca-R-P-P-G-F-S-A-F-K(Dnp)-OH by CatA was monitoring in a spectrofluorometer (Tecan®; Germany) at 330nm excitation and 390nm emission.

Statistical analysis - All data are expressed as mean±SD. Statistical analysis was carried out using Prism software (Graph Pad Version 7) or Progenesis® LC-MC software (Non-linear Dynamics) for proteomics. An unpaired Student's t-test (two-tailed) was used for statistical analyses comparing 2 groups. P-values of <0.05 and fold-change >2 (for proteomics) were considered statistically significant.

DATA AVAILABILITY

The mass spectrometry proteomics data have been deposited to the ProteomeXchange Consortium via the PRIDE [40] partner repository with the dataset identifier PXD019895 and 10.6019/PXD019895. All other data are contained within the article (and supplemental information).

ACKNOWLEDGMENTS

We thank Jeannette Zimolong, Nina Rebmann, Julia Weber, Sarah Triem and Claudia Noll for excellent technical support. We thank Sanofi for providing CatA-TG mice. This work was supported by: German Society of Cardiology (DGK0914), German Heart Foundation (F0315), Else-Kröner-Fresenius Foundation (2014A306), German Research Foundation (SFB TRR219-M02/M04/S02/C09/C02). Lisa Lang received a scholarship by the Stiftung Begabtenförderung berufliche Bildung (SBB) GmbH. Professor Manuel Mayr is a British

Heart Foundation (BHF) Chair Holder (CH/16/3/32406) with BHF programme grant support (RG/16/14/32397) and member of a network on “Defining the Roles of Smooth Muscle Cells and Other Extracellular Matrix Producing Cells in Late Stage Atherosclerotic Plaque Pathogenesis” funded by the Foundation Leducq.

CONFLICT OF INTEREST

The authors declare no competing financial interests. Sven Ruf, Thomas Hübschle and Thorsten Sadowski are employees of Sanofi-Aventis Deutschland GmbH.

REFERENCES

1. Souders CA, Bowers SL, Baudino TA. Cardiac fibroblast: the renaissance cell. *Circ Res*. 2009;**105**:1164-1176.
2. Müller AL, Dhalla NS. Role of various proteases in cardiac remodeling and progression of heart failure. *Heart Fail Rev*. 2012;**17**:395-409.
3. Cheng XW, Shi GP, Kuzuya M, Sasaki T, Okumura K, Murohara T. Role for cysteine protease cathepsins in heart disease: focus on biology and mechanisms with clinical implication. *Circulation*. 2012;**125**:1551-1562.
4. Everts V, van der Zee E, Creemers L, Beertsen W. Phagocytosis and intracellular digestion of collagen, its role in turnover and remodeling. *Histochem J*. 1996;**28**:229-245.
5. Timur ZK, Akyildiz Demir S, Seyrantepe V. Lysosomal Cathepsin A Plays a Significant Role in the Processing of Endogenous Bioactive Peptides. *Front Mol Biosci*. 2016;**3**:68.
6. Jackman HL, Massad MG, Sekosan M, Tan F, Brovkovich V, Marcic BM, Erdos EG. Angiotensin 1-9 and 1-7 release in human heart: role of cathepsin A. *Hypertension*. 2002;**39**:976-981.
7. Hiraiwa M. Cathepsin A/protective protein: an unusual lysosomal multifunctional protein. *Cell Mol Life Sci*. 1999;**56**:894-907.
8. Zhou XY, Galjart NJ, Willemsen R, Gillemans N, Galjaard H, d'Azzo A. A mutation in a mild form of galactosialidosis impairs dimerization of the protective protein and renders it unstable. *EMBO J*. 1991;**10**:4041-4048.
9. Seyrantepe V, Hinek A, Peng J, Fedjaev M, Ernest S, Kadota Y, Canuel M, Itoh K, Morales CR, Lavoie J, Tremblay J, Pshezhetsky AV. Enzymatic activity of lysosomal carboxypeptidase (cathepsin) A is required for proper elastic fiber formation and inactivation of endothelin-1. *Circulation*. 2008;**117**:1973-1981.
10. Ruf S, Buning C, Schreuder H, Horstick G, Linz W, Olpp T, Pernerstorfer J, Hiss K, Kroll K, Kannt A, Kohlmann M, Linz D, Hübschle T, Rütten H, Wirth K, Schmidt T, Sadowski T. Novel β -amino acid derivatives as inhibitors of cathepsin A. *J Med Chem*. 2012;**55**:7636-7649.
11. Linz D, Hohl M, Dhein S, Ruf S, Reil JC, Kabiri M, Wohlfart P, Verheule S, Böhm M, Sadowski T, Schotten U. Cathepsin A mediates susceptibility to atrial tachyarrhythmia and impairment of atrial emptying function in Zucker diabetic fatty rats. *Cardiovasc Res*. 2016;**110**:371-380.
12. Hohl M, Erb K, Lang L, Ruf S, Hübschle T, Dhein S, Linz W, Elliott AD, Sanders P, Zamyatkin O, Böhm M, Schotten U, Sadowski T, Linz D. Cathepsin A Mediates Ventricular Remote Remodeling and Atrial Cardiomyopathy in Rats With Ventricular Ischemia/Reperfusion. *JACC Basic Transl Sci*. 2019;**4**:332-344.
13. Petrera A, Gassenhuber J, Ruf S, Gunasekaran D, Esser J, Shahinian JH, Hübschle T, Rütten H, Sadowski T, Schilling O. Cathepsin A inhibition attenuates myocardial infarction-induced heart failure on the functional and proteomic levels. *J Transl Med*. 2016;**14**:153.
14. Abonnenc M, Nabeebaccus AA, Mayr U, Barallobre-Barreiro J, Dong X, Cuello F, Sur S, Drozdov I, Langley SR, Lu R, Stathopoulou K, Didangelos A, Yin X, Zimmermann WH, Shah AM, Zampetaki A, Mayr M. Extracellular matrix secretion by cardiac fibroblasts: role of microRNA-29b and microRNA-30c. *Circ Res*.

- 2013;**113**:1138-1147.
15. Petersen SV, Oury TD, Ostergaard L, Valnickova Z, Wegrzyn J, Thøgersen IB, Jacobsen C, Bowler RP, Fattman CL, Crapo JD, Enghild JJ. Extracellular superoxide dismutase (EC-SOD) binds to type I collagen and protects against oxidative fragmentation. *J Biol Chem.* 2004;**279**:13705-13710.
 16. Park SK, Kim J, Seomun Y, Choi J, Kim DH, Han IO, Lee EH, Chung SK, Joo CK. Hydrogen peroxide is a novel inducer of connective tissue growth factor. *Biochem Biophys Res Comm.* 2001;**284**:966-971.
 17. Sirker A, Zhang M, Shah AM. NADPH oxidases in cardiovascular disease: insights from in vivo models and clinical studies. *Basic Res Cardiol.* 2011;**106**:735-747.
 18. Sivakumar P, Gupta S, Sarkar S, Sen S. Upregulation of lysyl oxidase and MMPs during cardiac remodeling in human dilated cardiomyopathy. *Mol Cell Biochem.* 2008;**307**:159-167.
 19. Frangogiannis NG. The extracellular matrix in myocardial injury, repair, and remodeling. *J Clin Invest.* 2017;**127**:1600-1612.
 20. Dong Fan, Abhijit Takawale, Jiwon Lee, Zamaneh Kassiri. Cardiac fibroblasts, fibrosis and extracellular matrix remodeling in heart disease. *Fibrogenesis Tissue Repair.* 2012;**5**:15.
 21. Jackman HL, Tan FL, Tamei H, Beurling-Harbury C, Li XY, Skidgel RA, Erdös EG. A peptidase in human platelets that deamidates tachykinins. Probable identity with the lysosomal "protective protein". *J Biol Chem.* 1990;**265**:11265-11272.
 22. Brömme D., Wilson S. (2011) Role of Cysteine Cathepsins in Extracellular Proteolysis. In: Parks W., Mecham R. (eds) Extracellular Matrix Degradation. Biology of Extracellular Matrix, vol 2. Springer, Berlin, Heidelberg; doi.org/10.1007/978-3-642-16861-1_2
 23. Almeida PC, Nantes IL, Chagas JR, Rizzi CC, Faljoni-Alario A, Carmona E, Juliano L, Nader HB, Tersariol IL. Cathepsin B activity regulation. Heparin-like glycosaminoglycans protect human cathepsin B from alkaline pH-induced inactivation. *J Biol Chem.* 2001;**276**:944-951.
 24. Olsen DA, Petersen SV, Oury TD, Valnickova Z, Thøgersen IB, Kristensen T, Bowler RP, Crapo JD, Enghild JJ. The intracellular proteolytic processing of extracellular superoxide dismutase (EC-SOD) is a two-step event. *J Biol Chem.* 2004;**279**:22152-22157.
 25. Kliment CR, Oury TD. Extracellular superoxide dismutase protects cardiovascular syndecan-1 from oxidative shedding. *Free Radic Biol Med.* 2011;**50**:1075-1080.
 26. Lu Z, Xu X, Hu X, Zhu G, Zhang P, van Deel ED, French JP, Fassett JT, Oury TD, Bache RJ, Chen Y. Extracellular superoxide dismutase deficiency exacerbates pressure overload-induced left ventricular hypertrophy and dysfunction. *Hypertension.* 2008;**51**:19-25.
 27. van Deel ED, Lu Z, Xu X, Zhu G, Hu X, Oury TD, Bache RJ, Duncker DJ, Chen Y. Extracellular superoxide dismutase protects the heart against oxidative stress and hypertrophy after myocardial infarction. *Free Radic Biol Med.* 2008;**44**:1305-1313.
 28. Kliment CR, Suliman HB, Tobolewski JM, Reynolds CM, Day BJ, Zhu X, McTiernan CF, McGaffin KR, Piantadosi CA, Oury TD. Extracellular superoxide dismutase regulates cardiac function and fibrosis. *J Mol Cell Cardiol.* 2009;**47**:730-742.
 29. Dewald O, Frangogiannis NG, Zoerlein M, Duerr GD, Klemm C, Knuefermann P, Taffet G, Michael LH, Crapo JD, Welz A, Entman ML. Development of murine ischemic cardiomyopathy is associated with a transient inflammatory reaction and depends on reactive oxygen species. *Proc Natl Acad Sci U S A.* 2003;**100**:2700-2705
 30. Petrera A, Kern U, Linz D, Gomez-Auli A, Hohl M, Gassenhuber J, Sadowski T, Schilling O. Proteomic Profiling of Cardiomyocyte-Specific Cathepsin A Overexpression Links Cathepsin A to the Oxidative Stress Response. *J Proteome Res.* 2016 Sep

- 2;15(9):3188-95. doi: 10.1021/acs.jproteome.6b00413.
31. Barallobre-Barreiro J, Gupta SK, Zoccarato A, Kitazume-Taneike R, Fava M, Yin X, Werner T, Hirt MN, Zampetaki A, Viviano A, Chong M, Bern M, Kourliouros A, Domenech N, Willeit P, Shah AM, Jahangiri M, Schaefer L, Fischer JW, Iozzo RV, Viner R, Thum T, Heineke J, Kichler A, Otsu K, Mayr M. Glycoproteomics Reveals Decorin Peptides With Anti-Myostatin Activity in Human Atrial Fibrillation. *Circulation*. 2016;**134**:817-832.
 32. Yin X, Cuello F, Mayr U, Hao Z, Hornshaw M, Ehler E, Avkiran M, Mayr M. Proteomics analysis of the cardiac myofilament subproteome reveals dynamic alterations in phosphatase subunit distribution. *Mol Cell Proteomics*. 2010;**9**:497-509.
 33. Barallobre-Barreiro J, Didangelos A, Schoendube FA, Drozdov I, Yin X, Fernández-Caggiano M, Willeit P, Puntmann VO, Aldama-López G, Shah AM, Doménech N, Mayr M. Proteomics analysis of cardiac extracellular matrix remodeling in a porcine model of ischemia/reperfusion injury. *Circulation*. 2012;**125**:789–802.
 34. Zafiriou MP, Noack C, Unsöld B, Didie M, Pavlova E, Fischer HJ, Reichardt HM, Bergmann MW, El-Armouche A, Zimmermann WH, Zelarayan LC. Erythropoietin responsive cardiomyogenic cells contribute to heart repair post myocardial infarction. *Stem Cells*. 2014;**32**:2480-2491.
 35. Zafeiriou MP, Noack C and Laura Cecilia Zelarayan. Isolation and Primary Culture of Adult Mouse Cardiac Fibroblasts. *BioProtoc*.1860; Vol 6, Iss 13, 7/5/2016
 36. DeChiara TM, Poueymirou WT, Auerbach W, Frendewey D, Yancopoulos GD, Valenzuela DM. Producing fully ES cell-derived mice from eight-cell stage embryo injections. *Methods in Enzymology*. 2010;**476**:285-293.
 37. Reil JC, Hohl M, Reil GH, Granzier HL, Kratz MT, Kazakov A, Fries P, Müller A, Lenski M, Custodis F, Gräber S, Fröhlig G, Steendijk P, Neuberger HR, Böhm M. Heart rate reduction by If-inhibition improves vascular stiffness and left ventricular systolic and diastolic function in a mouse model of heart failure with preserved ejection fraction. *Eur Heart J*. 2013;**34**:2839-2849.
 38. Nickel AG, von Hardenberg A, Hohl M, Löffler JR, Kohlhaas M, Becker J, Reil JC, Kazakov A, Bonnekoh J, Stadelmaier M, Puhl SL, Wagner M, Bogeski I, Cortassa S, Kappl R, Pasiaka B, Lafontaine M, Lancaster CR, Blacker TS, Hall AR, Duchon MR, Kästner L, Lipp P, Zeller T, Müller C, Knopp A, Laufs U, Böhm M, Hoth M, Maack C. Reversal of Mitochondrial Transhydrogenase Causes Oxidative Stress in Heart Failure. *Cell Metab*. 2015;**22**:472-484.
 39. Nagaraju CK, Dries E, Popovic N, Singh AA, Haemers P, Roderick HL, Claus P, Sipido KR, Driesen RB. Global fibroblast activation throughout the left ventricle but localized fibrosis after myocardial infarction. *Sci Rep*. 2017;**7**:10801.
 40. Perez-Riverol Y, Csordas A, Bai J, Bernal-Llinares M, Hewapathirana S, Kundu DJ, Inuganti A, Griss J, Mayer G, Eisenacher M, Pérez E, Uszkoreit J, Pfeuffer J, Sachsenberg T, Yilmaz S, Tiwary S, Cox J, Audain E, Walzer M, Jarnuczak AF, Ternent T, Brazma A, Vizcaíno JA. The PRIDE database and related tools and resources in 2019: improving support for quantification data. *Nucleic Acids Res* 2019;**47**(D1):D442-D450

FIGURES AND TABLES

Figure 1

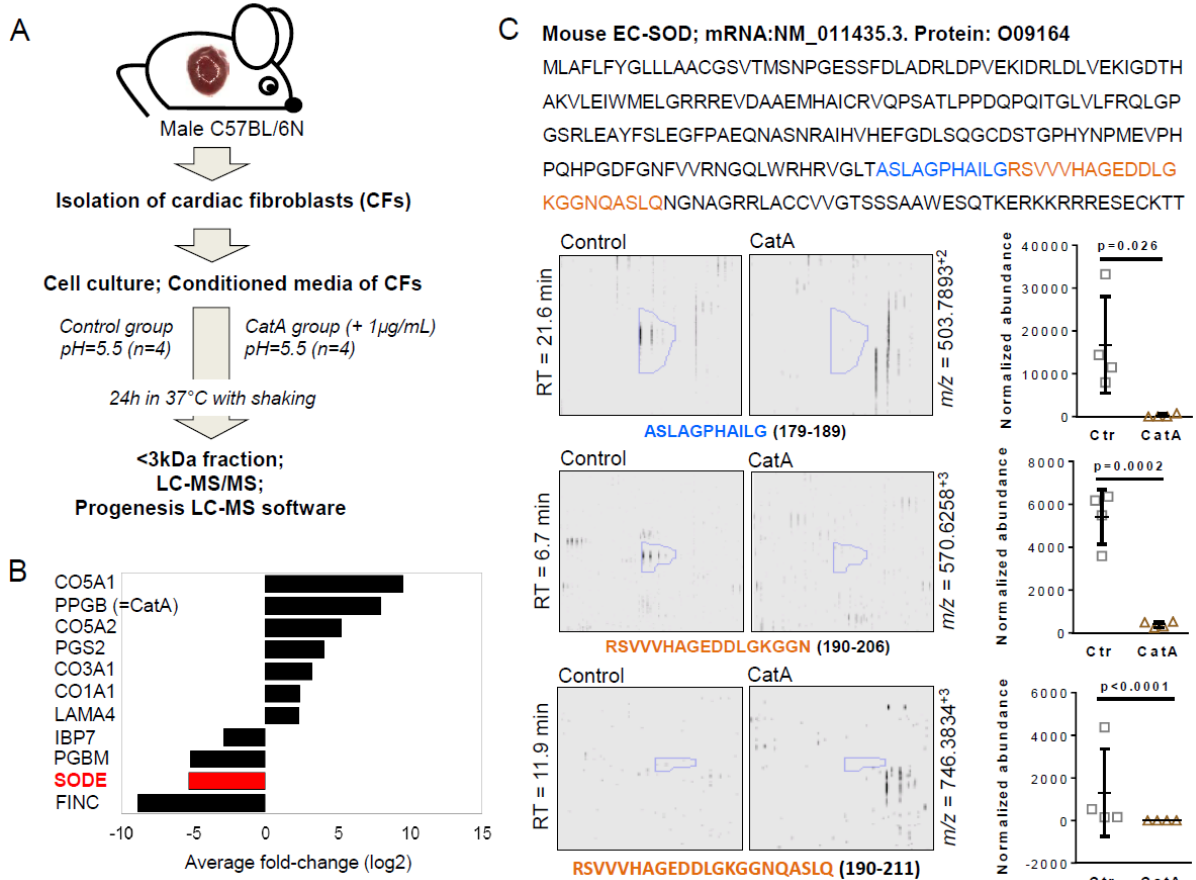


Figure 1: Proteomics of cathepsin A (CatA) degradation products in conditioned media from cardiac fibroblasts (CFs). (A) Proteomics-workflow of degradation products in conditioned media from CFs after digestion with CatA. Isolation and culture of primary mouse CFs: Primary mouse CFs were isolated from the hearts of male C57BL/6N mice (n=4). For secretome analysis, 80% confluent CFs were cultured in serum-free medium for 3 days. The secreted proteins from the conditioned media were either incubated with human recombinant CatA (1µg/mL) or without (control group) in assay buffer (pH5.5). Degradation products in the <3kDa fractions were analyzed by LC-MS/MS and significantly changed peptides (>2-fold intensity change, p<0.05) were identified by Mascot (Matrix Science; version 2.3.01) in a no-enzyme search against the UniProt/SwissProt mouse database. (B) Proteins with differential abundance in the conditioned medium after filtering using 3kDa columns to recover protein fragments (collagens (CO5A1, CO5A2, CO3A1, CO1A1), Decorin (PGS2), Laminin Subunit Alpha 4 (LAMA4), Basement membrane-specific heparan sulfate proteoglycan core protein (PGBM), Fibronectin (FINC) and extracellular superoxide dismutase (SODE or EC-SOD). (C) Three peptides were detected for EC-SOD. The Figures display the retention time (RT, y-axis) versus the mass-to-charge ratio (m/z, x-axis) for the three EC-SOD peptides. Quantification based on normalized abundance is shown for each of the peptides (n=4 per group). All values are presented as mean±SD.

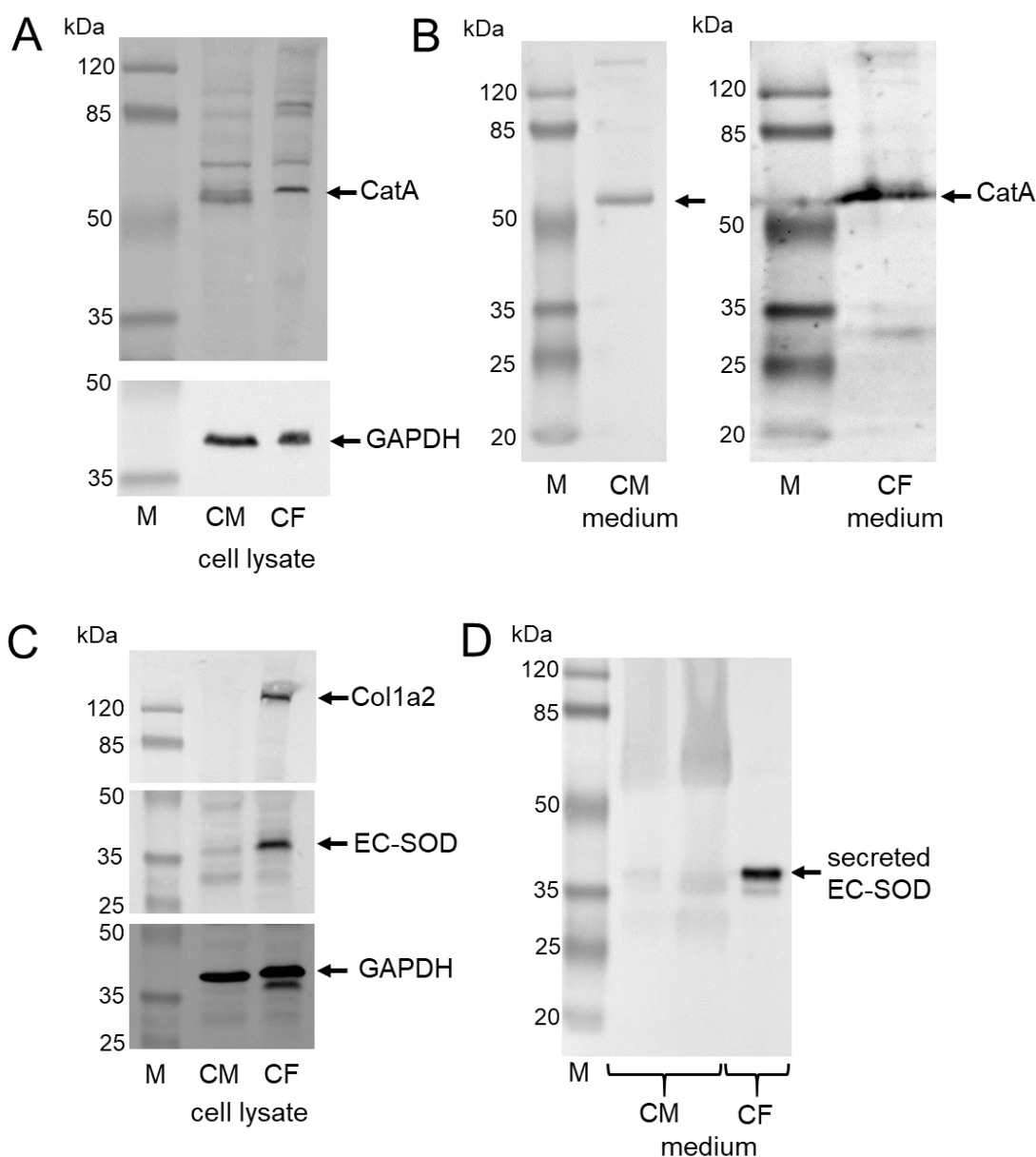
Figure 2

Figure 2: Differential expression and secretion of cathepsin A (CatA) and extracellular superoxide dismutase (EC-SOD) by cardiomyocytes (CMs) and cardiac fibroblasts (CFs). CMs and CFs were isolated from 4-6 days old Sprague Dawley rats with mixed sex. **(A)** Western blot analysis demonstrating cellular protein expression of CatA in isolated neonatal CMs and in CFs. Glyceraldehyde 3-phosphate dehydrogenase (GAPDH) served as loading control of cell lysates. **(B)** Western blot analysis of secreted CatA protein comparing serum-free cell culture medium derived from CM and CF after 48 hours. **(C)** Western blot analysis of EC-SOD protein in isolated CMs and CFs. Collagen 1a2 (Col1a2) protein served as fibroblast-specific control and Glyceraldehyde 3-phosphate dehydrogenase (GAPDH) served as loading control of cell lysates. **(D)** Western blot analysis of secreted EC-SOD protein comparing serum-free cell culture medium derived from CMs and CFs after 48 hours.

Figure 3

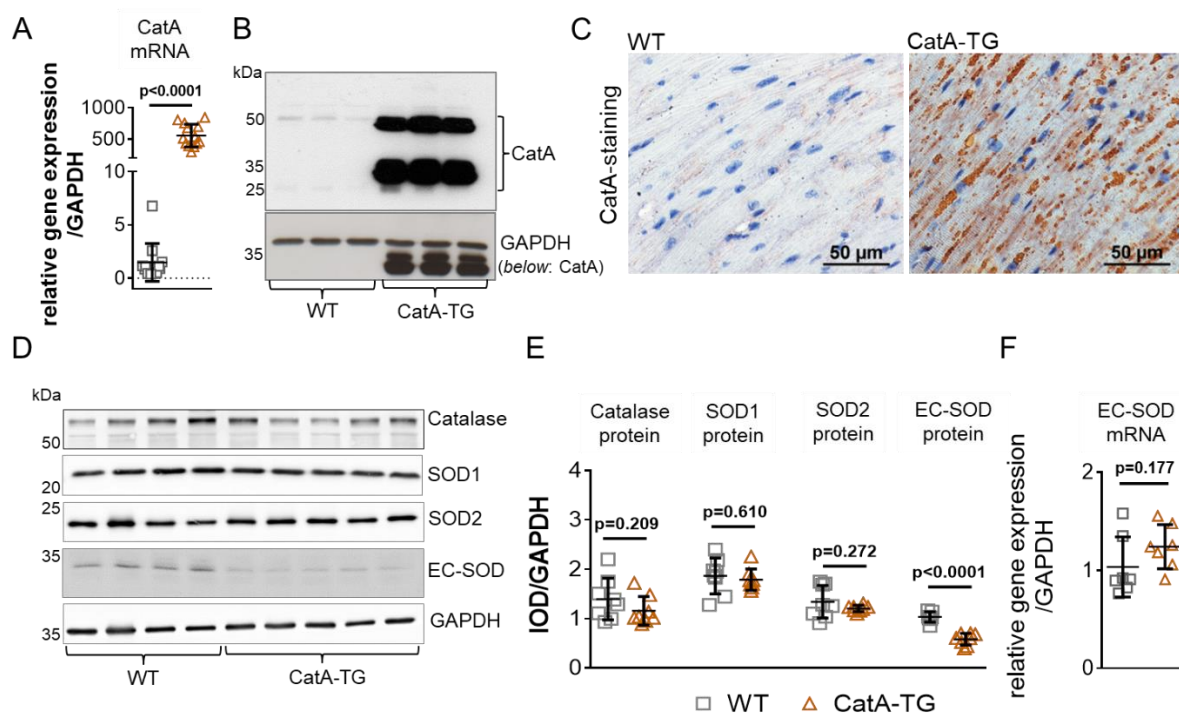


Figure 3: Cardiomyocyte-specific overexpression of cathepsin A (CatA) effects extracellular superoxide dismutase (EC-SOD) processing. (A) Left ventricular (LV) expression of human CatA mRNA and (B) protein in male 6-month-old mice with cardiomyocyte-specific overexpression of human CatA (CatA-TG) and their wild type littermates (WT). (C) Representative images of LV tissue immunohistologically stained for overexpressed human CatA. (D) Representative Western blot and quantification (E) of protein expression of catalase, superoxide dismutase 1 (SOD1), SOD2 and extracellular SOD (EC-SOD) in LV tissue of CatA-TG mice (n=8) and their wild type littermates (WT, n=7-8) as well as (F) mRNA expression of EC-SOD (n=7 per group). All values are presented as mean \pm SD.

Figure 4

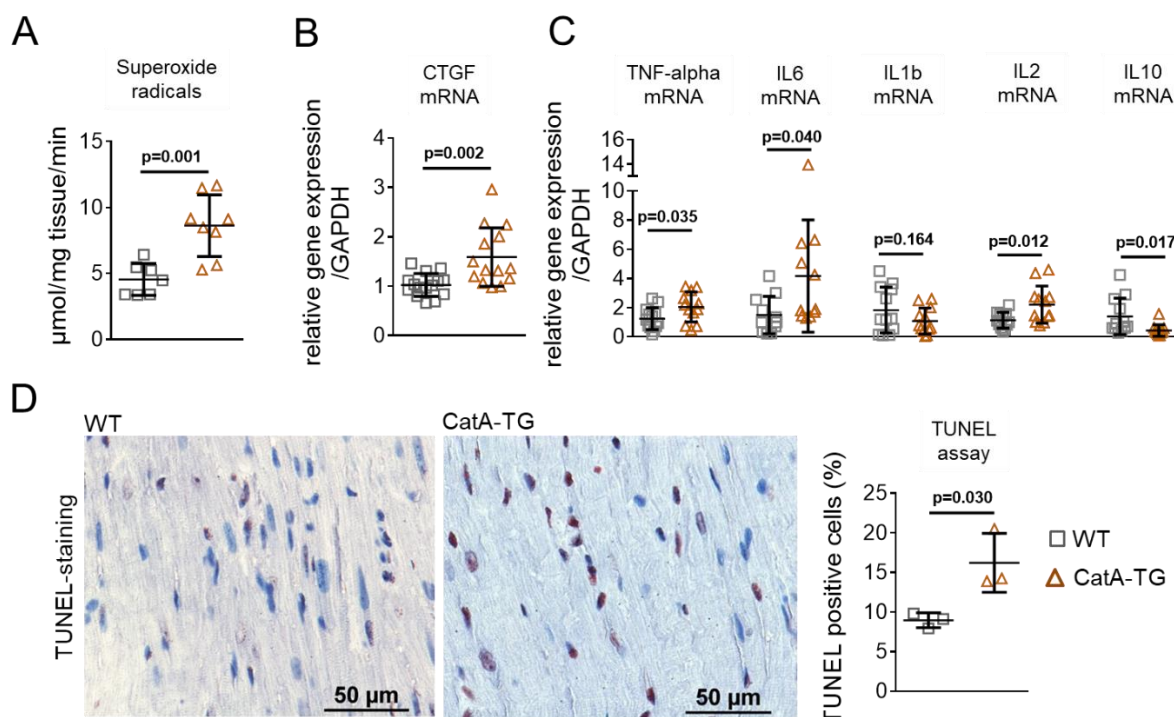


Figure 4: Impact of cardiomyocyte-specific cathepsin A (CatA) overexpression on the cellular oxidative stress and inflammation. (A) Analysis of superoxide radical production (n=7-8 per group) in LV tissue of WT and CatA-TG as well as (B) mRNA expression of redox-sensitive connective tissue growth factor (CTGF) (n=14 per group). (C) Real-Time PCR quantification of pro-inflammatory marker genes tumor necrosis factor alpha (TNF α (WT n=13, CatA n=12)), interleukin 6 (IL6; n=11 per group), interleukin 1 beta (IL1b; n=12 per group), and interleukin 2 (IL2; n=12 per group) as well as anti-inflammatory interleukin 10 (IL10; n=12 per group). (D) Assessment of apoptosis by quantification of TUNEL positive cells in LV tissue of WT and CatA-TG (n=3 per group). All values are presented as mean \pm SD.

Figure 5

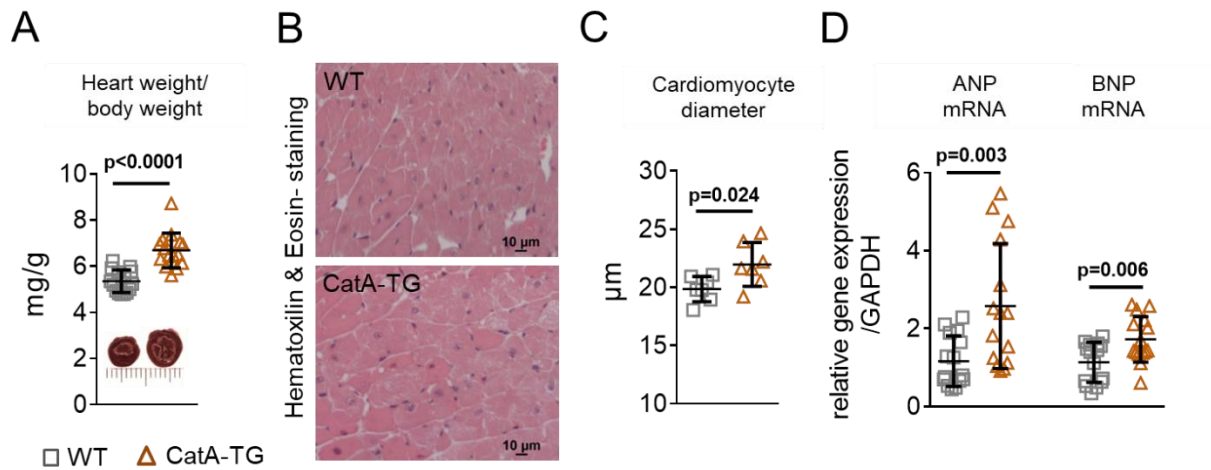


Figure 5: Cardiomyocyte-specific overexpression of cathepsin A (CatA) and cardiac hypertrophy. (A) Heart weight to body weight ratio (n=15 per group). (B) Representative images used for histological analysis and (C) quantification of cardiomyocyte diameter (n=7 per group). (D) mRNA expression of hypertrophy marker genes atrial natriuretic peptide (ANP) and brain natriuretic peptide (BNP) in WT and CatA-TG mice (n=15 per group). All values are presented as mean \pm SD.

Figure 6

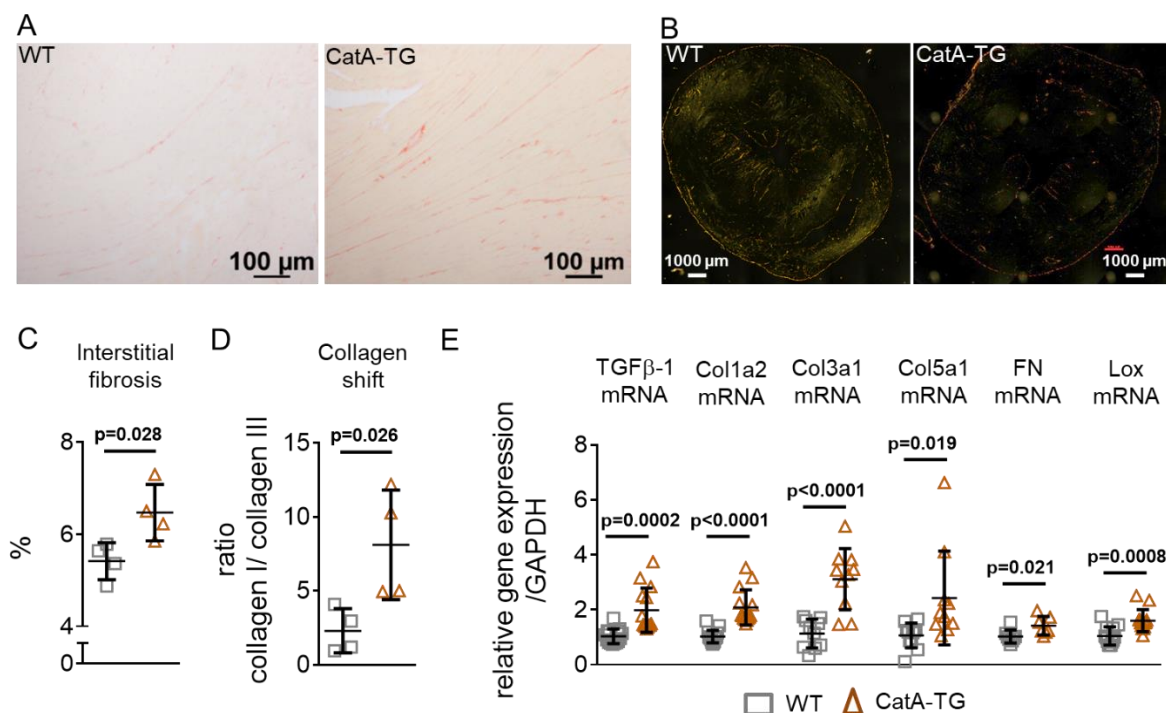


Figure 6: Cardiomyocyte-specific overexpression of cathepsin A (CatA) causes left ventricular (LV) interstitial remodeling. (A) Representative images used for histological analysis and (B) Polarized light microscopy Picro-Sirius Red stained left ventricular preparations to visualizes collagen type I (red-yellow fibers) and collagen type III (green fibers). (C) Quantification of LV interstitial fibrosis amount (n=4 per group). (D) Quantification of collagen type I to collagen type III ratio. (E) Transcription levels of profibrotic gene transforming growth factor beta (TGF β), of collagens Col1a2, Col1a3 and Col5a1, fibronectin (FN), and lysyl oxidase (Lox) in WT and CatA-TG. (C) All values are presented as mean \pm SD.

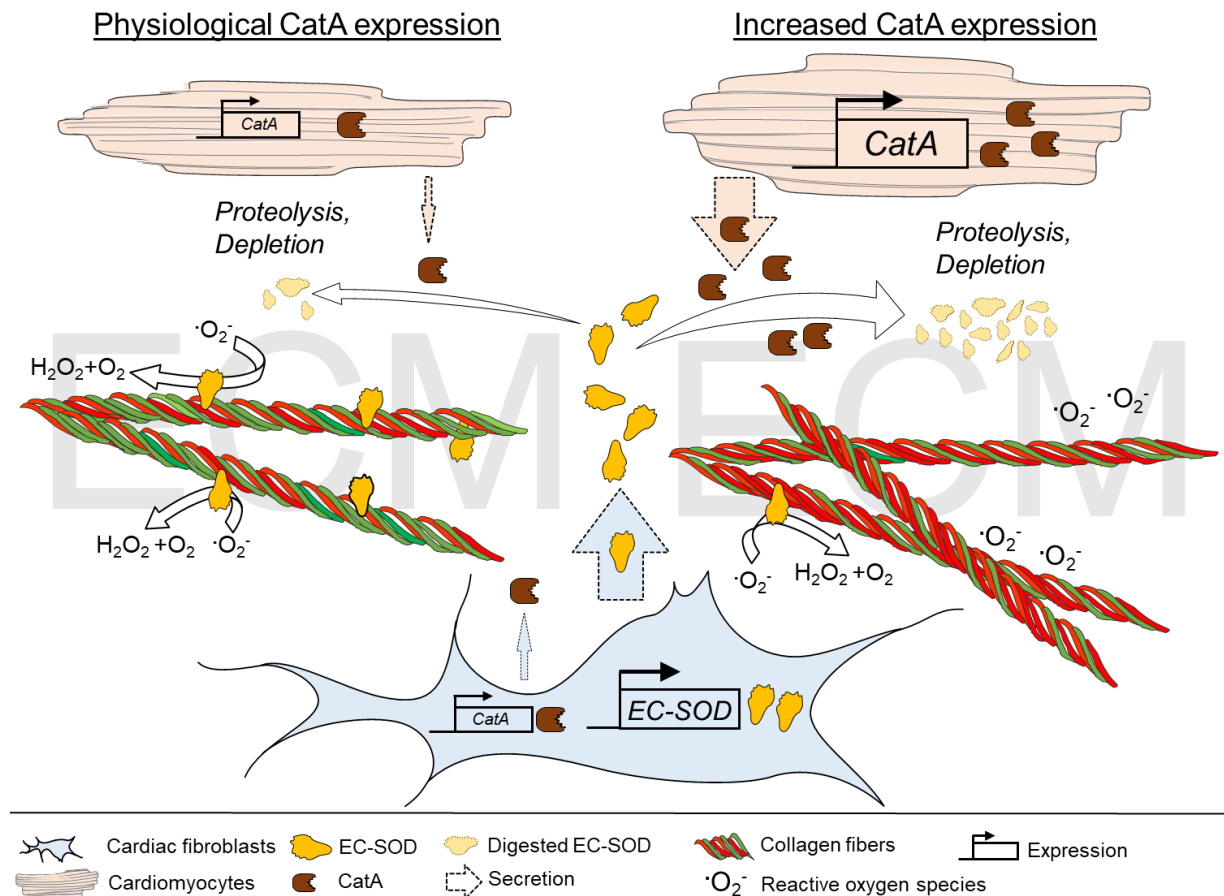


Figure 7: Summary. The antioxidant enzyme extracellular superoxide dismutase (EC-SOD) is expressed and secreted in abundance into the extracellular matrix (ECM) by cardiac fibroblasts (CFs). In the ECM, EC-SOD protects against reactive oxygen species by dismutation of $\cdot\text{O}_2^-$ to H_2O_2 and O_2 . The carboxypeptidase cathepsin A (CatA) is expressed by both CFs and cardiomyocytes (CMs) and secreted into the extracellular space where it proteolytically degrades EC-SOD, thereby regulating EC-SOD distribution in the ECM. Cardiomyocyte-specific overexpression of CatA leads to enhanced EC-SOD protein degradation and accelerated depletion from the ECM, subsequently increasing vulnerability to reactive oxygen species followed by cardiac fibrosis formation with a higher quantity of collagen type I fibers (red fibers) and myocardial hypertrophy.

	WT (n=5)	CatA-TG (n=5)	p-Value
EF [%]	51.4±19.2	51.4±6.3	p=0.998
LVEDV [μl]	50.8±5.8	61.9±6.2	p=0.018
LVESV [μl]	25.2±12.0	29.8±3.4	p=0.434
SV [μl]	25.6±7.5	32.1±6.3	p=0.172
HR [bpm]	397±16	402±41	p=0.812
dP/dt max [mmHg/sec]	4980.8±1782.0	4913.6±565.0	p=0.937
dP/dt min [mmHg/sec]	-3446.6±782.3	-3670.8±493.4	p=0.602
CO [μl/min]	10.2±3.1	13.0±3.2	p=0.206
Tau-weiss [msec]	14.2±4.2	11.9±1.9	p=0.298
Endsystolic pressure [mmHg]	67.6±6.4	70.9±4.7	p=0.381
Enddiastolic pressure [mmHg]	7.7±3.5	7.6±2.5	p=0.952

Table 1: Hemodynamic characterization of cathepsin A (CatA) transgenic mice in the working heart apparatus. Cardiac function was characterized in six months old CatA transgenic mice (CatA-TG) and their wild type littermates (WT) using an isolated working heart apparatus. Ejection fraction (EF), left ventricular end-diastolic volume (LVEDV), left ventricular end-systolic volume (LVESV), stroke volume (SV), heart rate (HR), LV contractility (dP/dtmax) and relaxation (dP/dtmin), cardiac output (CO). All values are presented as mean±SD

Cathepsin A contributes to left ventricular remodeling by degrading extracellular superoxide dismutase in mice

Mathias Hohl, Manuel Mayr, Lisa Lang, Alexander G. Nickel, Javier Barallobre Barreiro, Xiaoke Yin, Thimoteus Speer, Simina Ramona Selejan, Claudia Goettsch, Katharina Erb, Claudia Fecher-Trost, Jan-Christian Reil, Benedikt Linz, Sven Ruf, Thomas Hübschle, Christoph Maack, Michael Böhm, Thorsten Sadowski and Dominik Linz

J. Biol. Chem. published online July 9, 2020

Access the most updated version of this article at doi: [10.1074/jbc.RA120.013488](https://doi.org/10.1074/jbc.RA120.013488)

Alerts:

- [When this article is cited](#)
- [When a correction for this article is posted](#)

[Click here](#) to choose from all of JBC's e-mail alerts